



Sea Ice CCI+



ESA CCI+ CLIMATE CHANGE INITIATIVE
PHASE 1: NEW R&D ON CCI ECVS

Contract number:
4000126449/19/I-NB



High(er) Resolution SEA ICE CONCENTRATION (SICCI-HR-SIC)

PRODUCT USER GUIDE (PUG)

Reference: D4.2

Issue: 3.0


Date: 17 February 2023



Max-Planck-Institut
für Meteorologie



UNIS
The University Centre in Svalbard

 <p>Norwegian Meteorological Institute</p>	<p>The Norwegian Meteorological Institute (METNO) Henrik Mohns Plass 1 N-0313 Oslo Norway Phone: + 47 22 96 30 00 Fax: + 47 22 96 30 50 E-Mail: thomas.lavergne@met.no http://www.met.no</p>
--	---

<p>Contract PHASE 1 OF THE CCI+ CLIMATE CHANGE INITIATIVE NEW R&D ON CCI ECVs SEA ICE ECV</p>	<p>Deliverable D4.2 Product User Guide</p>
<p>CLIENT European Space Agency</p>	<p>CLIENT REFERENCE 4000126449/19/I-NB</p>
<p>Revision date: 17 February 2023</p>	
<p>Principal Authors <i>Atle M. Sørensen, Norwegian Meteorological Institute</i> <i>Thomas Lavergne, Norwegian Meteorological Institute</i></p>	

Change Record

Issue	Date	Reason for Change	Author(s)
1.0	03.03.2020	First version	Atle Sørensen
2.0	30.11.2020	Second version	Atle Sørensen, Thomas Lavergne
2.1	11.02.2021	Minor updates addressing RIDs from ESA TO	Thomas Lavergne
3.0	17.02.2023	Third version for public release	Thomas Lavergne and Atle Sørensen

Document Approval

Role	Name	Signature
Written by:	T. Lavergne	
Edited by:	M. A. Killie	
Approved by:	A. M. Trofaier	

Contents

1 INTRODUCTION.....	5
1.1 Purpose.....	5
1.2 Scope.....	5
1.3 Document Status.....	5
1.4 Reference documents.....	5
1.5 Acronyms and Abbreviations.....	5
1.6 Executive Summary.....	6
2 Dates with artifacts.....	8
3 Input data.....	8
3.1 The SSM/I data.....	9
3.2 The SSMIS data.....	11
3.3 Numerical Weather Prediction data.....	11
3.4 The EUMETSAT OSI SAF Sea Ice Concentration CDR v3.....	11
3.5 Binary land mask.....	11
3.6 Sea Ice Extent Climatology.....	13
4 Processing scheme.....	14
5 Product description.....	15
5.1 Product specification.....	15
5.2 Grid specification.....	20
5.3 Meta data specification.....	21
5.4 File naming convention.....	21
5.5 Product access.....	22
6 Known limitations.....	22
7 References.....	24
8 Appendix A: Missing dates.....	26

1 INTRODUCTION

1.1 Purpose

This document is the Product User Guide for SICCI-HR-SIC the High(er) Resolution Sea Ice Concentration (SIC) Climate Data Record from the Sea Ice ECV CCI+ PHASE 1 - NEW R&D ON CCI ECVs activity, which is being undertaken by a METNO-led consortium.

1.2 Scope

The Product User Guide describes how the CDR files are structured, and how to use them, as well as briefly describing the processing chain and known limitations.

1.3 Document Status

This is the third release of this PUG, the first public release to document SICCI-HR-SIC.

1.4 Reference documents

This is the Product User Guide (PUG) for SICCI-HR-SIC. Reference documents are:

- [RD-1] Sea Ice Concentration Algorithm Theoretical Basis Document (ATBD) for the ESA CCI datasets, D2.1, revision 3.1, available from the DOI landing page.
- [RD-2] High(er) Resolution Sea Ice Concentration Product Validation and Intercomparison Report (PVIR), D4.1, revision 3.1, available from the DOI landing page.
- [RD-3] EUMETSAT OSI SAF Algorithm Theoretical Baseline Document (ATBD) for the Global Sea Ice Concentration Climate Data Records v3 (OSI-450-a, OSI-430-a, OSI-458), SAF/OSI/CDOP3/DMI_Met/SCI/MA/270, version v3.0, August 2022, available from <https://osi-saf.eumetsat.int/products/osi-450-a>

1.5 Acronyms and Abbreviations

The table below lists the acronyms and abbreviations used in this volume.

Acronym	Meaning
C3S	Copernicus Climate Change Service
CCI	Climate Change Initiative
CDR	Climate Data Record
DMSP	Defence Meteorological Satellite Program
EASE2 grid	Equal-Area Scalable Earth Grid v2
ECMWF	European Centre for Medium-Range Weather Forecasts
ESA	European Space Agency
EUMETSAT	European Organization for the Exploitation of Meteorological Satellites
FCDR	Fundamental Climate Data Record
FoV (<i>alt</i> FOV)	Field-of-View
FYI	First Year Ice
ICDR	Interim Climate Data Record
L1B, L2, L3, ...	Satellite data processing Level (Level-1b, ...)
MYI	Multi-Year Ice
NSIDC	US National Snow and Ice Data Centre
NWP	Numerical Weather Prediction
OSI SAF	EUMETSAT Ocean and Sea Ice Satellite Application Facility
OWF	Open Water Filter
PMR	Passive Microwave Radiometer
PMW	Passive Microwave
RTM	Radiative Transfer Model
SIC	Sea Ice Concentration
SSM/I	Special Sensor Microwave/Imager
SSMIS	Special Sensor Microwave Imager/Sounder
SSMIs	Both SSM/I and SSMIS sensors

Table 1: Acronyms and Abbreviations. Acronyms for the deliverable items (URD, etc...) and partner institutions (AWI,..) are not repeated.

1.6 Executive Summary

The High(er) Resolution Sea Ice Concentration Climate Data Record from ESA CCI (SICCI-HR-SIC) is a global dataset covering 30 years (1991-2020). It is processed from passive microwave imagery and Numerical Weather Prediction data through a dedicated algorithm.

SICCI-HR-SIC is an **advanced pan-sharpened version of OSI-450-a**, the most recent SIC CDR from the EUMETSAT OSI SAF. This advanced pan-sharpening approach required specific R&D and algorithms to be conducted in the CCI+ Sea Ice Phase 1 project, and

resulted in a standalone dataset which is **higher resolution but shorter** than the dataset from OSI SAF. Note that ESA CCI+ Sea Ice Phase 1 also contributed R&D input to the OSI SAF processing chains.

SICCI-HR-SIC uses the high-frequency, high(er) resolution near-90 GHz imagery of the SSM/I and SSMIS satellite missions to obtain higher resolution SIC fields (12.5 km) than OSI-450-a (25 km). Such near-90 GHz imagery has only been available since 1991.

We briefly introduce the main input and auxiliary data used and the processing methodology. We then document the file format (main variables, uncertainty fields, etc...) and how to access the SICCI-HR-SIC data. We finally remind of known limitations with such passive microwave SIC data records.

This Product User Guide is one of the user's document released together with the SICCI-HR-SIC CDR. Two other user's documents are the Algorithm Theoretical Basis Document (ATBD, RD-1) and the Product Intercomparison and Validation Report (PVIR, RD-2).

2 Dates with artifacts

Despite our careful examination before the release of SICCI-HR-SIC, there might still be artefacts in some of the product files. We encourage our users to contact us if they find such artefacts, so that they can be listed in this section.

Readers are also referred to section 6 for a more general description of known limitations with the product.

3 Input data

This chapter describes the SSM/I and SSMIS satellite data, as well as numerical weather prediction (NWP) data, used for the SICCI-HR-SIC CDR. Figure 1 shows a timeline of the satellite missions having relevant passive microwave sensors, many of which enter our SIC CDR.

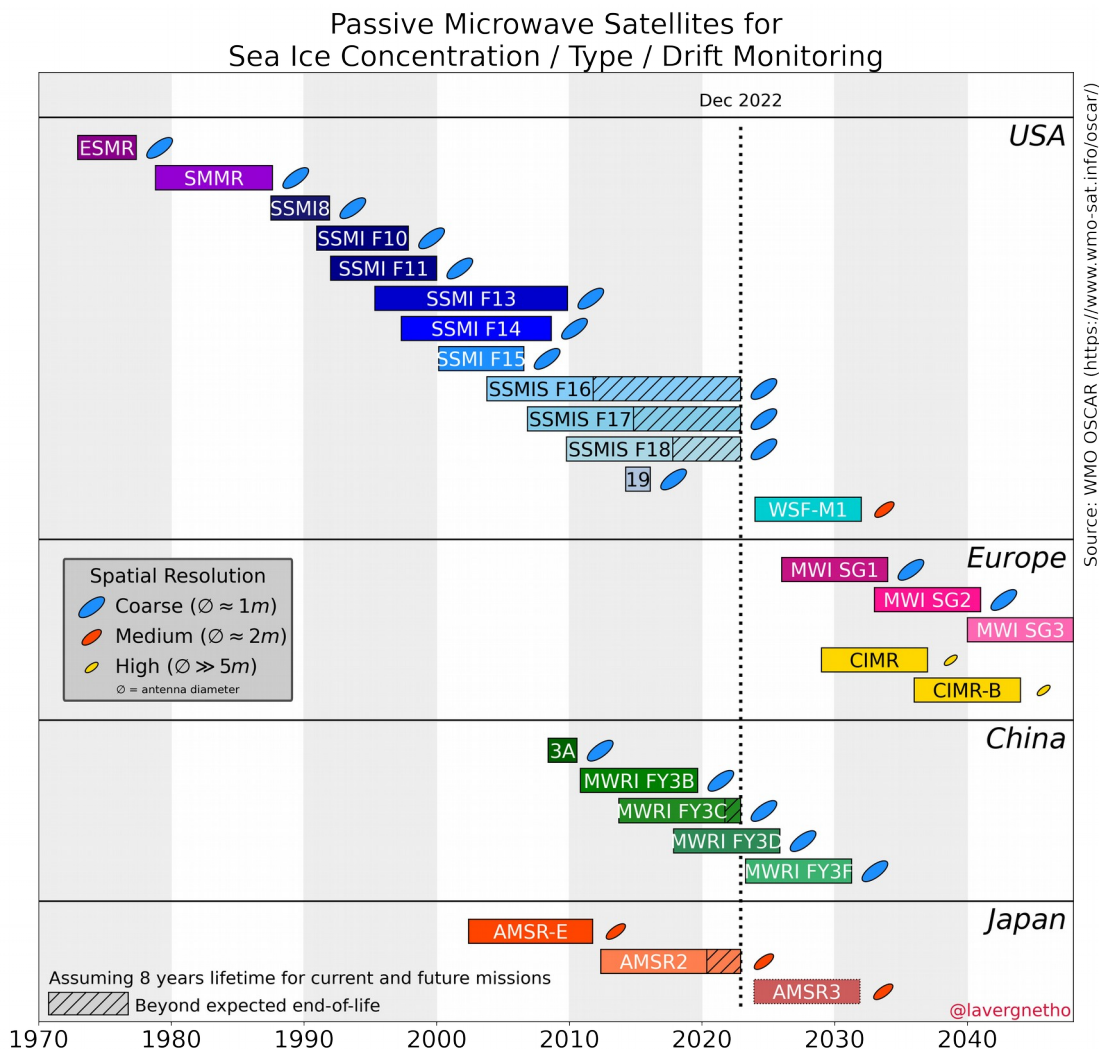


Figure 1: Timeline of the Passive Microwave satellite missions relevant for sea-ice concentration/extent/area monitoring (as well as Type and Drift) with an indication of their spatial resolution capabilities. The horizontal bars represent satellite missions, which are colored by sensor family. The SICCI-HR-SIC CDR uses the SSM/I (F10 onwards) and all SSMIS.

3.1 The SSM/I data

The Special Sensor Microwave/Imager (SSM/I) sensors on board the Defence Meteorological Satellite Program (DMSP) satellites started its record with the F08 satellite on 9th July 1987, shortly before the SMMR ceased to operate. The SSM/I is a total power radiometer, with a conical scan measuring the upwelling radiation from the Earth at a constant incidence angle of about 53.1° at four frequencies (19.3, 22.2, 37.0, 85.5 GHz). The swath width is about 1400 km and the polar observation hole extends to 87° .

The SSM/I data set used for this reprocessing was prepared by EUMETSAT CM SAF (Release 4, http://doi.org/10.5676/EUM_SAF_CM/FCDR_MWI/V004) and covers the period

of available DMSP satellite instruments from 1991 to 2008 (F10, F11, F13, F14, F15) (see Table 2). Some SSM/I instruments continued their mission further than 2008, but these data are not included in the CM SAF FCDR.

The SSM/I instruments have five low-frequency channels (19 GHz to 37 GHz). In addition, two higher-frequency channels at 85 GHz, with twice the sampling rate and better spatial resolution, are available on the SSM/I starting with DMSP F10 (the 85 GHz channels had a malfunction on F08). Characteristics of the SSM/I imagery channels are listed in Table 3.

Satellite	Period covered
F08	Not used because of early failure of the 85 GHz imagery.
F10	Jan 1991 - Nov 1997
F11	Jan 1992 – Dec 1999
F13	May 1995 – Dec 2008
F14	May 1997 – Aug 2008
F15	Feb 2000 – Jul 2006

Table 2: The different satellite missions carrying the SSM/I instrument and the periods they cover.

Frequency (GHz)	Polarizations	Sampling	Footprint size	
			Along-track	Cross-track
19.35	H,V	25 km	69 km	43 km
22.235	V	25 km	50 km	40 km
37.0	H,V	25 km	37 km	28 km
85.5	H,V	12.5 km	15 km	13 km

Table 3: Characteristics of the different SSM/I channels.

Readers interested in the processing, calibration and quality check steps applied in the FCDR will find many more details in the CM-SAF documentation and Fennig et al. (2020).

3.2 The SSMIS data

The SSMIS instruments are a slight evolution of the SSM/I concept, and most characteristics that drive the design of SIC CDRs are similar to SSM/I. Noticeable differences are the smaller polar observation hole (89°), and the center frequency of the high-frequency channels (91.1 GHz). The SSMIS instruments were also on board DMSP satellites, and we use F16, F17, and F18 missions (F19 was a short-lived mission, and F20 was never launched). DMSP F18 is thus the last available SSMIS instrument.

Data from three DMSP platforms are used in the CDR SICCI-HR-SIC: F16 (Nov 2005 - Dec 2013), F17 (Dec 2006 - Dec 2020), and F18 (Mar 2010 - Dec 2020). They are from CM SAF FCDR (Release 4, http://doi.org/10.5676/EUM_SAF_CM/FCDR_MWI/V004).

3.3 Numerical Weather Prediction data

The microwave radiation emitted by the ocean and sea ice travels through the Earth's atmosphere before being recorded by the satellite sensors. Scattering, reflection, and emission in the atmosphere add or subtract contributions to the radiated signal, and challenge our ability to accurately quantify sea-ice concentration.

A central step in our Level-2 processing is thus the explicit correction of the T_b for the atmospheric contribution to the top of the atmosphere radiation. For this purpose, we use global hourly fields from the C3S ERA5 reanalysis (produced by ECMWF, see Hersbach et al., 2020). Fields of 10m wind speed, 2m air temperature, total column water vapour and total column cloud liquid water are used.

3.4 The EUMETSAT OSI SAF Sea Ice Concentration CDR v3

As described in section 1.6 and 4, the present High(er) Resolution Sea Ice Concentration CDR from ESA CCI (SICCI-HR-SIC) is a pan-sharpened version of the SIC CDR from EUMETSAT OSI SAF v3 (OSI-450-a, http://dx.doi.org/10.15770/EUM_SAF_OSI_0013). The OSI SAF SIC products we used are themselves based on SSM/I and SSMIS missions (from the 19 and 37 GHz imagery) and use ERA5 NWP fields.

Links to OSI-450-a documentation and data are on <https://osi-saf.eumetsat.int/products/osi-450-a>.

3.5 Binary land mask

Land masks for the target 12.5×12.5 km grids (one for NH and one for SH) are prepared from two higher resolution sources. The ocean mask is from the ESA SST CCI OSTIA L4 product (version 2.1), at 0.05×0.05° resolution (~6x3 km in the polar regions). The lake mask is from the ESA Lakes CCI (ESACCI-LAKES_mask_v1.nc) at 0.0083×0.0083° (~1x0.5 km in the

polar regions). The OSTIA L4 land mask is selected because of the long tradition of preparing SST+SIC analyses. We have also investigated other land masks (such as that of the ESA CCI Land Cover project, but it did not make a difference at these spatial scales.

These high-resolution binary masks are first regridded to the EASE2 12.5×12.5 km NH and SH grids to prepare “density_of_land”, “density_of_ocean”, and “density_of_lakes” variables (all 3 in [0,1] and the sum equals 1). The Caspian Sea, which is a water body both in the SST and lakes mask, is considered a lake for our Sea Ice Concentration CDR.

Then, a binary “smask” (surface mask) variable is prepared from the three density_of_* fields. Variable “smask” takes on values "0: ocean, 1: ocean coastline, 2: land, 4: lake coastline, 5: lake" (see Figure 2). In the final product, sea-ice concentration values are provided for all grid cells with smask 0 (ocean) and 5 (lakes).

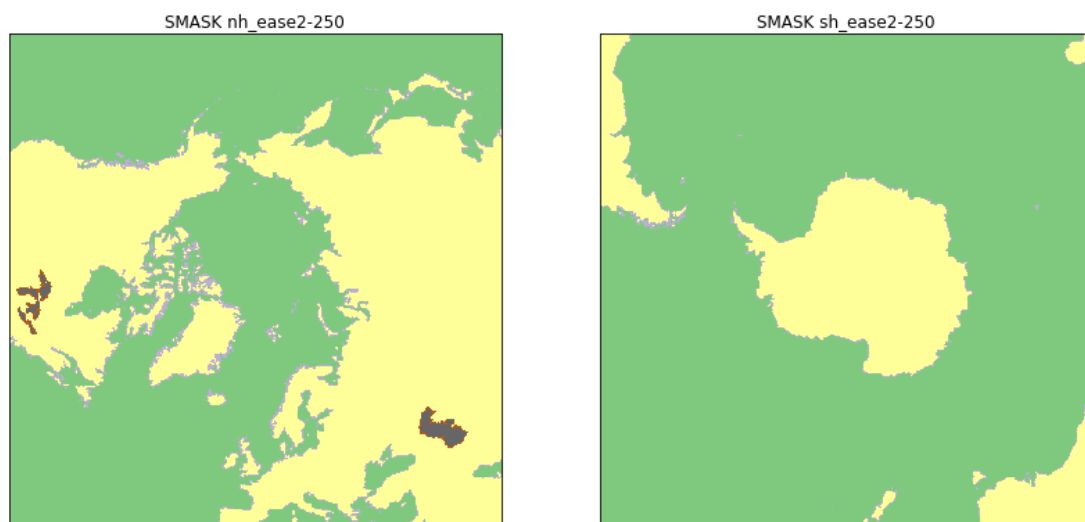


Figure 2: Variable "smask" used in SICCI-HR-SIC on the EASE2 12.5 km grids (left: NH, right: SH). Ocean (smask=0): green, Ocean coastline (smask=1): light grey, Land (smask=2): yellow, Lake coastline (smask=4): red, Lake (smask=5): dark grey.

As for the OSI SAF v3 SIC CDRs, it was decided to only keep the largest lake systems (Caspian Sea and the US Great Lakes) for SICCI-HR-SIC, and not to consider smaller inland water (e.g. Great Bear Lake, Baikal, Ladoga).

The SICCI-HR-SIC mask (at 12.5 km spacing) is cross-checked against the OSI-450-a mask (at 25 km spacing). In particular, 2x2 cells of SICCI-HR-SIC mask are forced to being “land” where the corresponding OSI-450-a mask is “land”. This is to ensure that we do not introduce too narrow straits or fjords at 12.5 km that are not resolved (no data) in OSI-450-a as this would lead to too much extrapolation of OSI-450-a.

3.6 Sea Ice Extent Climatology

We use the same monthly varying maximum sea-ice extent climatology as in OSI-450-a. This is used to filter out grossly erroneous sea-ice detection far from the polar regions, and along the coastlines at mid to high latitudes. A monthly varying climatology is required because of the large seasonal variability of the polar sea ice extent.

The monthly varying maximum sea-ice extent climatology implemented in the NSIDC SIC CDR v3 (Peng et al. 2013 , Meier et al., 2017) was used as a basis for our climatology. The NSIDC climatology is described in their Climate-ATBD (available from the dataset landing page of Meier et al., 2017) and covers the years up-until 2007.

We then did some modifications to the climatologies, mainly manual editing of some single pixels, based on US National Ice Center, Canadian Ice Service, and Norwegian and Finnish Ice Service ice charts (e.g. along the coast of northern Norway, for some summer months in the vicinity of Nova Scotia and in the Baltic Sea and Gulf of Finland). The climatology of peripheral seas and large freshwater bodies (e.g. Bohai and Northern Yellow Seas, Great Lakes, Caspian Sea, and Sea of Azov) was also revisited.

In developing the “v3” climatology, a focus has been on the coastal regions during summer, especially the Baltic Sea. These coastal regions are still challenging for the SICCI-HR-SIC because of land spill-over. We liaised with the Finnish Ice Service and adapted the regional climatology using their input.

The cleaned climatologies are then expanded with a buffer zone of 150 km in the NH and 250 km in the SH. This expansion is not applied in the Baltic Sea during summer months. The larger expansion in SH is to cope with the slight positive trends in the SH sea-ice extent (Parkinson, 2019).

Although SICCI-HR-SIC covers a shorter period than OSI-450-a, we chose to use exactly the same climatology for both CDRs to increase the consistency between the two sources.

4 Processing scheme

The Algorithm Theoretical Basis Document (ATBD) [RD-1] contains all the details of the algorithms and processing steps involved in the production of SICCI-HR-SIC from SSM/I and SSMIS imagery data, ERA5 NWP fields, and the OSI-450-a CDR.

Figure 3 summarizes the two main processes involved: a) preparing a higher resolution, higher uncertainty SIC field with an N90LIN algorithm and RTM-based correction of the brightness temperatures, and b) using this N90LIN SIC field to sharpen the low resolution, low uncertainty OSI-450-a SIC.

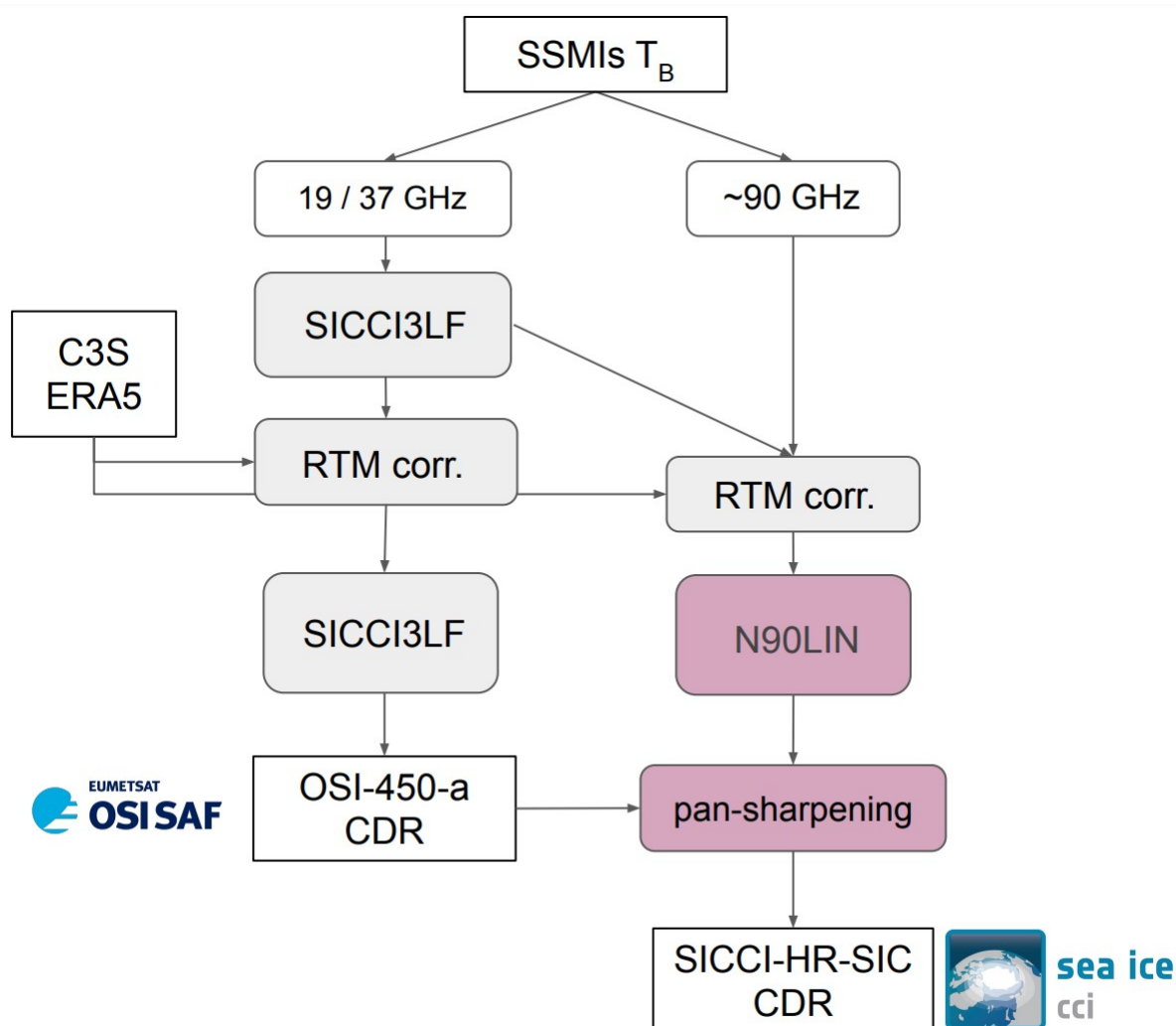


Figure 3: Summary of the process to prepare the SICCI-HR-SIC: a high resolution, high uncertainty SIC field is prepared using an N90LIN algorithm and RTM correction of the T_B . This field is used to sharpen the low resolution, low uncertainty SIC from OSI-450-a.

The N90LIN SIC algorithm and the pan-sharpening algorithm are specific to the ESA CCI dataset, and are not used in OSI SAF. Note that ESA CCI+ Sea Ice Phase 1 contributed R&D

input to the OSI SAF processing chain, e.g. the SICCI3LF SIC algorithm.

5 Product description

This chapter gives a description of the product specification, meta data, data format and product availability. The file format is exactly the same as that used for OSI-450-a.

5.1 Product specification

The product files contain six variables (in addition to latitude, longitude, time, and other CF-related information):

- main (filtered) sea ice concentration (`ice_conc`)
- raw sea ice concentration values (`raw_ice_conc_values`)
- total uncertainty (`total_standard_uncertainty`)
- smearing uncertainty (`smearing_standard_uncertainty`)
- algorithm uncertainty (`algorithm_standard_uncertainty`)
- status flag (`status_flag`)

The definitions of these fields are given in the sections below. These fields are all covering the same grid.

For users of earlier (v2) OSI SAF or SICCI SIC CDRs, the only difference in variable names is that the three uncertainty variables are now named “_uncertainty” while they were (erroneously) named “_error” in v2.

Sea ice concentration (`ice_conc`)

Sea Ice Concentration is the fraction of the sea surface covered by sea ice. It is reported here in percentage, with a range from 0% to 100%. This variable holds sea-ice concentration maps after several filters (e.g. the open water filter) and post-processing steps (e.g. interpolation and thresholding) have been applied. It is the main variable for users of this Climate Data Record.

Examples are shown in Figure 4 and Figure 5. Figure 5 illustrates the greater level of details available from SICCI-HR-SIC (right) compared to OSI-450-a (left) thanks to the use of the high-frequency (near 90 GHz) imagery. SICCI-HR-SIC achieves similar details as OSI-458 (middle), the OSI SAF SIC CDR based on AMSR missions, and covers a longer period (30 years vs 20 years for OSI-458).

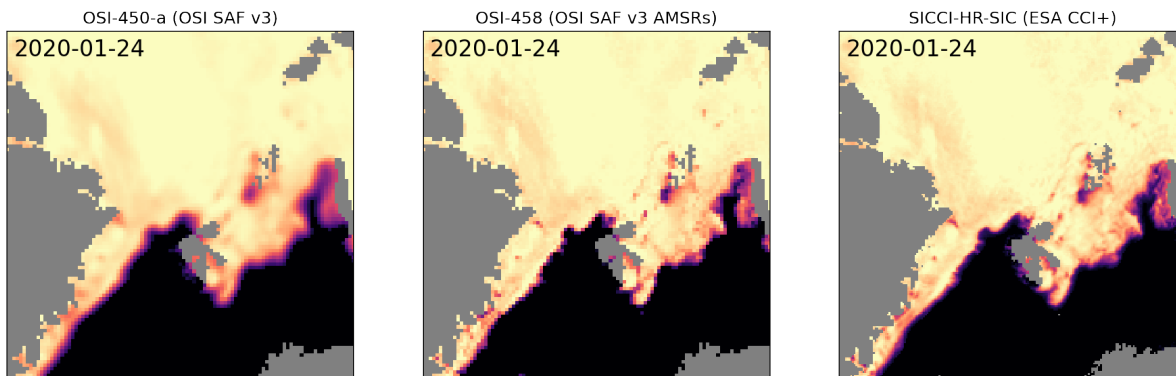
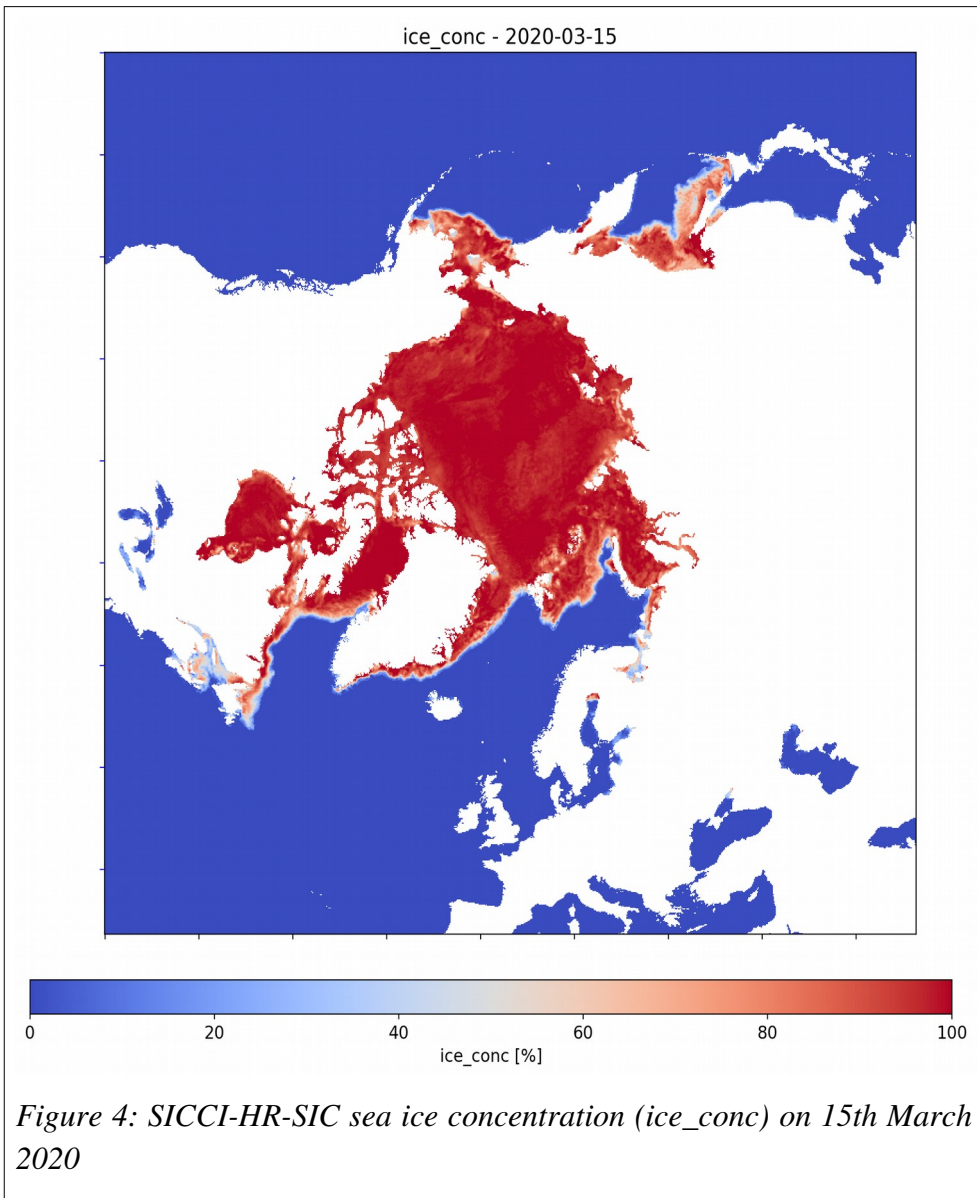


Figure 5: Comparison of SICCI-HR-SIC (right) with two OSI SAF CDRs for 2020-01-24.

Raw sea ice concentration values

Variable `raw_ice_conc_values` contains the original (“raw”) values of the sea ice concentration field, in cells where it has been altered during the filtering process in the level 4 step. For example, if the concentration was set to 0% in `ice_conc` due to the open water filter, then the original (raw) value will be available in `raw_ice_conc_values`. This variable is masked (with missing values) outside the maximum sea ice climatology and where the sea ice concentration is unaltered by the filters (in which case the sea-ice concentration value can be accessed from `ice_conc`). This variable can also contain un-physical ice concentration values such as values below 0% and above 100%. **This variable is for use by more advanced users**, who can take advantage of information with less filtering applied, e.g. via Data Assimilation techniques or for validation (Kern et al. 2019). An example can be seen in Figure 6.

`raw_ice_conc_values` must be used together with `ice_conc` to reconstruct the unfiltered field of sea-ice concentration values. This is a bit more work, but ensures that no user accesses full maps of unfiltered sea-ice concentrations (including values below 0% and above 100%) by accident.

A python snippet to reconstruct the full non-filtered sea-ice concentration field from variables `ice_conc`, `raw_ice_conc_values`, and `status_flags` is shown below.

```
import xarray as xr

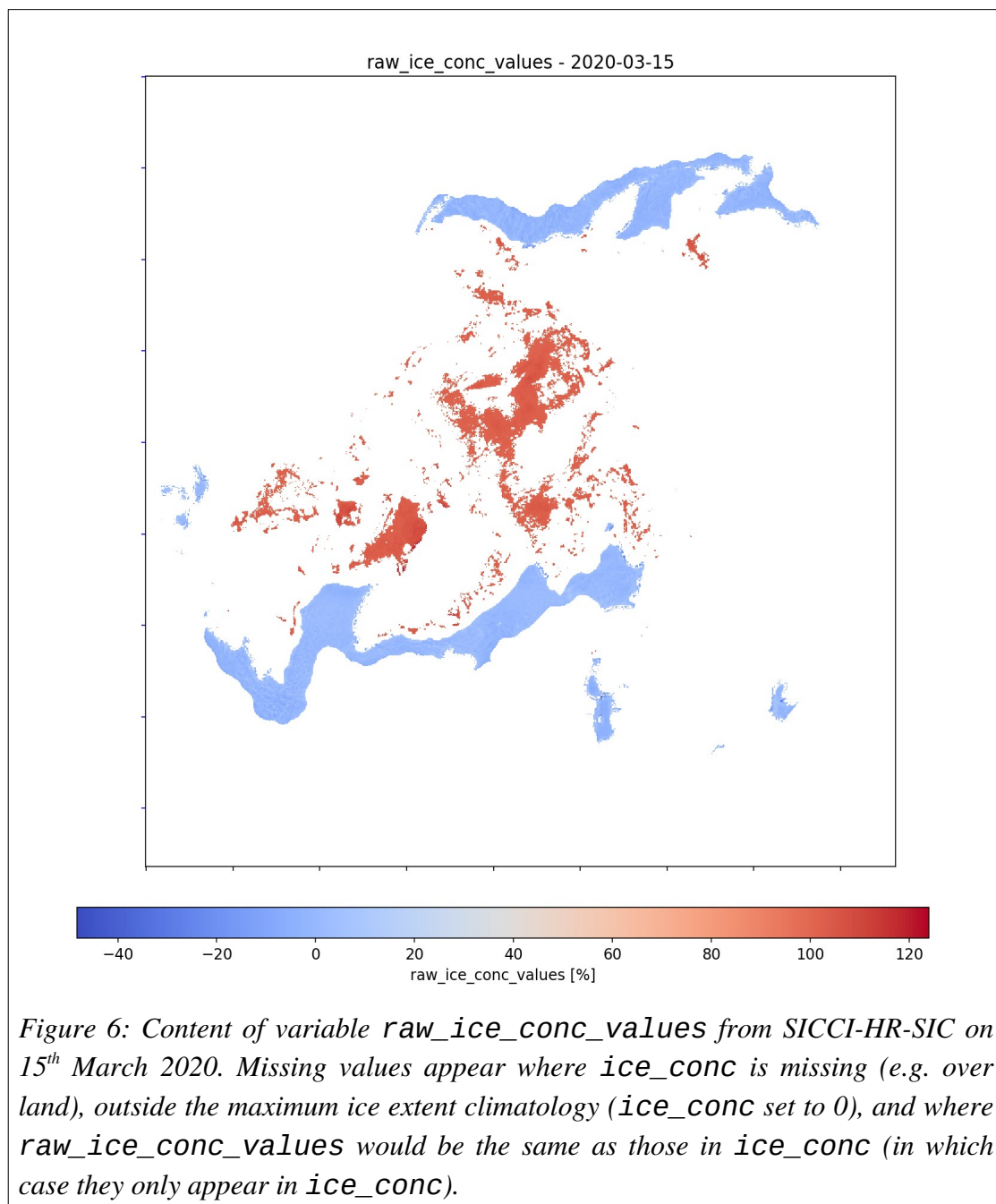
ds = xr.open_dataset(url_or_path_to_a_product_file)

ice_conc = ds['ice_conc'].to_masked_array()
raw_ice_conc_values = ds['raw_ice_conc_values'].to_masked_array()
status_flag = ds['status_flag'].to_masked_array().astype('short')

# combine ice_conc with raw_ice_conc_values using the status_flag
ice_conc[ice_conc==100] = raw_ice_conc_values[ice_conc==100]
ice_conc[(status_flag & 4) == 4] = raw_ice_conc_values[(status_flag & 4) == 4]

# ice_conc now holds the full non-filtered SIC field.
```

Code Example: Reconstructing the full non-filtered SIC field from `ice_conc`, `raw_ice_conc_values`, and `status_flags`.

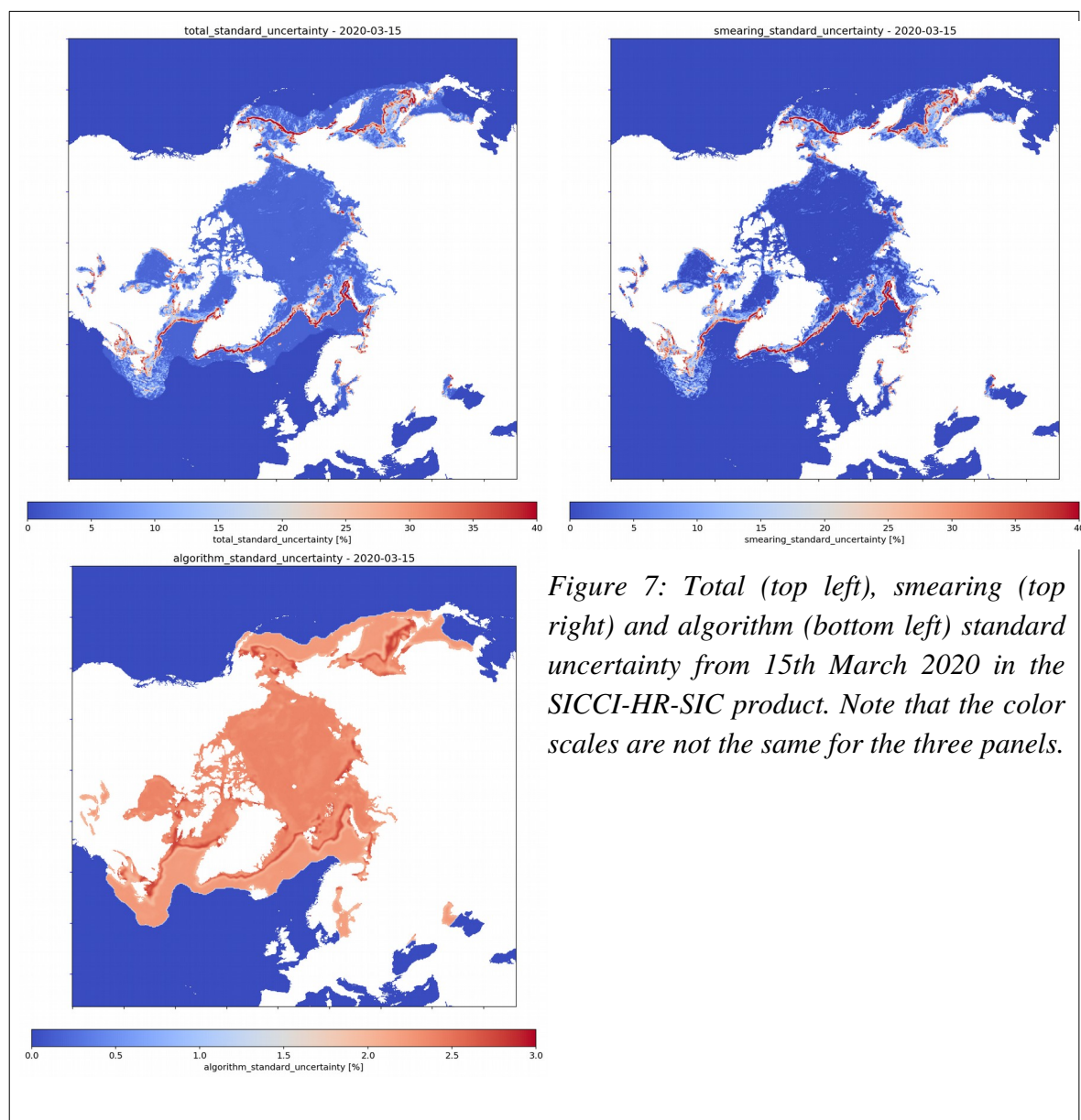


Uncertainty estimates

An estimate of the uncertainty of the sea ice concentration value in a grid cell is given in the separate *standard_uncertainty* fields. The uncertainty is given as one standard deviation in percentage. Three maps of uncertainty information are provided in each file, the algorithm standard uncertainty, the smearing standard uncertainty, and the total standard uncertainty. The total uncertainty is the combination (the square root of the sum of variances) of the two

other components of the uncertainty budget. An example is shown in Figure 7.

More details about the calculation of the uncertainty can be found in the ATBD [RD-1].



Status flag

The status flag contains information about the processing steps that have influenced the ice concentration value. It is coded as a signed character. The different values are described in Table 4.

Bit Nr	Value	Definition
1	1	Position is over land
2	2	Position is lake
3	4	SIC is set to zero by the open water filter
4	8	SIC value is changed for correcting land spill-over effects
5	16	Handle with caution, the 2m air temperature is high (≥ 5 degrees Celsius) at this position, and this might be false ice
6	32	Value is the result of spatial interpolation
7	64	Value is the result of temporal interpolation
8	128	SIC is set to zero since position is outside maximum sea ice climatology

Table 4: Definition of sea ice concentration status flag bits.

This value is a bit array with each bit representing a different status, so grid cell values can be a combination of several statuses. One example of this that may occur is an area where the concentration has been gap-filled using spatial interpolation, and where the open water filter kicks in setting the concentration to zero. This cell would then have the value 36 (a combination of the spatial interpolation (32) and open water filter (4) values).

Most combinations of flags are theoretically possible, with the exception of the 8th bit (outside maximum climatology) and first bit (over land) that both override other flags in the grid cells. Another excluded possibility is a combination of the third (open water filter) and fourth (land spill-over correction) bits, but this is due to their applicable areas not overlapping. Also, the value in a grid cell can't be both spatially and temporally interpolated.

5.2 Grid specification

For a given day, northern and southern hemisphere maps of sea ice concentration are available in two separate files. For both hemispheres, the sea ice concentration product is presented on a Lambert Azimuthal Equal Area polar projection, with a grid spacing of 12.5 km. The Lambert grid is also called the EASE2 grid, and is used by NSIDC for several of their sea ice and snow products. More documentation about the EASE2 grid can be found on their web site: <http://nsidc.org/data/ease/>.

The details of the grid definitions are given in Table 5 and illustrated on Figure 2. Projection definitions in the form of PROJ-4 initialization strings are also given.

Projection:	Lambert Azimuthal Equal Area (EASE2)
Resolution:	12.5 km
Size:	432 columns, 432 rows
Central Meridian:	0°
Datum/Earth:	WGS84 (a=6378137.0 m , b=6356752.314245 m)
Extent (corners of corner cells)	(-5400.0, -5400.0, +5400.0, +5400.0) [km]
PROJ-4 string:	NH: +proj=laea +ellps=WGS84 +datum=WGS84 +lat_0=90 +lon_0=0 SH: +proj=laea +ellps=WGS84 + datum=WGS84 +lat_0=-90 +lon_0=0

Table 5: Geographical definition for the EASE2 12.5 km grid, Northern and Southern Hemisphere.

The 12.5 km EASE2 grid of SICCI-HR-SIC is exactly aligned within the 25.0 km grid of OSI-450-a, so that 4 SICCI-HR-SIC grid cells cover exactly 1 OSI-450-a grid cell.

5.3 Meta data specification

The meta data included in the product file are given as NetCDF attributes to the variables and to the file (Global Attributes). Attributes associated to the variables are those required by the CF convention (<http://cfconventions.org/>), and all attributes follow the Attribute Convention for Data Discovery (ACDD) v1.3 ([http://wiki.esipfed.org/index.php/Attribute_Convention_for_Data_Discovery_\(ACDD\)](http://wiki.esipfed.org/index.php/Attribute_Convention_for_Data_Discovery_(ACDD))). NASA GCMD and IMO keywords were also selected.

5.4 File naming convention

The NetCDF/CF product files with daily SIC fields have the following naming convention:

ESACCI-SEAICE-L4-SICONC-RE_SSMI_12.5kmEASE2-<area>-<date8>-fv3.0.nc

where:

<area> : <NH> (Northern Hemisphere) and <SH> (Southern Hemisphere)

<date8> : central date of the analysis <YYYYMMDD>, e.g. 19911202.

5.5 Product access

The present ESA CCI+ High(er) Resolution Sea Ice Concentration CDR (SICCI-HR-SIC) covers the period from 01.01.1991 to 31.12.2020. Some periods and dates are missing due to missing satellite data. These dates are listed in Appendix A.

The data set is distributed freely through the ESA CCI Open Data Portal: climate.esa.int/data

6 Known limitations

Known limitations of the reprocessed sea ice concentration products are listed in this section. All the aspects listed apply in large extent to the other existing Sea Ice Concentration datasets based on Passive Microwave Radiometer (PMR) measurements. Users of the ESA CCI, OSI SAF, and other similar data sets should be fully aware of these so as not to bias their conclusions.

We also refer users to the dedicated Product Validation and Intercomparison Report (PVIR, RD-2) for validation statistics (RMSE, bias) for SICCI-HR-SIC, and comparison to other CDR, including those from OSI SAF.

Removal of true ice by the open water filters

The open water filter (aka weather filter) implemented in our SIC CDRs is based on combination of the PMR channels around 19 GHz and 37 GHz (Gloersen and Cavalieri, 1986). Although the filter is efficient at detecting and removing weather-induced noise over open water, it is also known to remove some amount of true low-concentration ice, especially in the marginal ice zone. The tuning of the open water filter is a trade-off between a) ensuring that no weather induced false ice is found in the maps and b) keeping the low range of true sea ice concentration as close to reality. It is also of prime importance that the open water filter is consistent throughout the time-series and across the changes of sensing frequencies (Kern et al., 2019).

For the SICCI-HR-SIC and OSI-450-a CDRs, a dynamic tuning of the filter was adopted. The tuning is done in such a way that the filter detects as open water (and thus sets 0% in the `ice_conc` variable) 1) all weather-induced false ice over ocean, and 2) potentially true sea ice up to 10% concentration. This 10% target is however only valid on average atmospheric conditions, and more compact ice might be affected by the filter as well (Andersen et al. 2006B; Ivanova et al. 2015).

The effect of the open water filter is not included in the uncertainty variables. The uncertainty variables are pertaining to the un-filtered (raw) ice concentration values. It is noted that the open water filters were slightly revised for the v3 CDRs (see OSI-450-a ATBD [RD-3]).

Summer melt and melt-ponding

Virtually all SIC algorithms based on the PMR channels around 19GHz, 37GHz, and 90GHz are very sensitive to surface melt and melt-pond water on top of the ice. In the early phase of melt, wet and warm snow has a higher emissivity than during winter (Kern et al., 2016). This change of emissivity before ponding is well captured by the dynamic tie-point approach implemented in our CDRs (Kern et al. 2020).

When melt-ponds appear on top of the ice, the radiation emitted at the microwave wavelengths used in SIC algorithms comes from a very thin water layer, which does not allow for distinguishing between ocean water (in leads) and melt water (in ponds). Based on these principles, the ice_conc variable of PMR SIC products should thus hold an estimate of 1 minus the open water fraction in each grid cell, irrespective if this water is from ocean or ponds (the net surface water fraction). However, Kern et al. (2020) recently showed that no existing PMR SIC data records performed satisfactorily during the melt season, neither in terms of true SIC, nor in terms of net surface water fraction.

The uncertainty variables in the OSI SAF SIC CDRs are larger during the summer melt seasons, even though the misinterpretation of melt-water as open water is not explicitly included in the uncertainty propagation. We have no reasons to believe that the SICCI-HR-SIC nor OSI-450-a CDRs will behave better or worse than the v2 CDRs during the summer melt season.

Thin and bare sea ice

Concentration of thin sea ice (< 30cm) is underestimated by most of the “classic” PMR SIC algorithms, due to the radiometric contribution of water below the ice to the signal. A complete, 100% cover of thin sea-ice, especially if it is predominantly bare (snow-free), indeed does not act as a radiometric insulator for the PMR frequencies around 19 and 37 GHz that are the base for this OSI SAF datasets, and many others. This is for example discussed in Ivanova et al. (2015).

The mis-interpretation of thin 100% sea ice coverage as ice with a lower concentration is not included in the uncertainty variables. We have no reasons to believe that the SICCI-HR-SIC nor OSI-450-a CDRs will behave better or worse than the v2 CDRs for thin sea ice conditions.

Interpolation of missing values

The SICCI-HR-SIC dataset aims at addressing needs from all users needing access to climate sea ice concentration data, from interested general public to climate modelers. It was decided to provide interpolated sea ice concentration values in places where original input satellite

data was missing, aiming at most complete daily maps. Both temporal and spatial interpolations are used. The locations where interpolation was used are clearly identified in the `status_flag` layer (see Table 4).

These interpolated sea ice concentration values should generally be used with caution for scientific applications, especially the values obtained from spatial interpolation. The uncertainty variables are not interpolated where data was missing.

The methodology for spatial interpolation was largely revised for OSI-450-a (and thus SICCI-HR-SIC) by adopting the algorithm of Strong and Golden (2016).

Coastal regions

The radiometric signature of land is similar to sea ice at the wavelengths used for estimating the SIC. Because of the large foot-prints and the relatively high brightness temperatures of land and ice compared to water, the land signature is “spilling” into the coastal zone open water and it will falsely look as intermediate concentration ice. Thanks to the better resolution of the near-90 GHz imagery of SSMIs missions, there should be less land-spillover effects for SICCI-HR-SIC than for OSI-450-a.

The land-spill-over effect is corrected for as described in the OSI-450-a ATBD [RD-3]. However, this coastal correction procedure is not perfect, and a level of false sea-ice remains along some coastlines. The uncertainty variables have larger values in the coastal regions where land spill-over effects are detected.

Fresh and brackish water ice

The retrieval of fresh and brackish water lake ice concentration is challenging when using coarse resolution microwave imagery. First, ice concentration retrievals suffer from land spill-over effects. Second, the microwave emissivity of lake ice is different from that of sea ice and would require specific algorithm tie-points. In the SICCI-HR-SIC, we purposely removed many small and medium lakes with our land mask (Figure 2) to reduce the issue but still call for caution when using the ice concentration values over lakes (as identified in the `status_flag`, Table 4).

7 References

- Andersen, S., R. Tonboe, S. Kern, and H. Schyberg. Improved retrieval of sea ice total concentration from spaceborne passive microwave observations using Numerical Weather Prediction model fields: An intercomparison of nine algorithms. *Remote Sensing of Environment* 104, 374-392, 2006B.
- Fennig, K., Schröder, M., Andersson, A., and Hollmann, R.: A Fundamental Climate Data

- Record of SMMR, SSM/I, and SSMIS brightness temperatures, *Earth Syst. Sci. Data*, 12, 647–681, <https://doi.org/10.5194/essd-12-647-2020>, 2020.
- Gloersen, P., and D. J. Cavalieri (1986), Reduction of weather effects in the calculation of sea ice concentration from microwave radiances, *J. Geophys. Res.*, 91(C3), 3913–3919, doi:[10.1029/JC091iC03p03913](https://doi.org/10.1029/JC091iC03p03913).
- Ivanova, N., Pedersen, L. T., Tonboe, R. T., Kern, S., Heygster, G., Lavergne, T., Sørensen, A., Saldo, R., Dybkjær, G., Brucker, L., and Shokr, M.: Inter-comparison and evaluation of sea ice algorithms: towards further identification of challenges and optimal approach using passive microwave observations, *The Cryosphere*, 9, 1797–1817, doi:10.5194/tc-9-1797-2015, 2015.
- Kern, S., Rösel, A., Pedersen, L. T., Ivanova, N., Saldo, R., and Tonboe, R. T.: The impact of melt ponds on summertime microwave brightness temperatures and sea-ice concentrations, *The Cryosphere*, 10, 2217–2239, doi:10.5194/tc-10-2217-2016, 2016.
- Kern, S., Lavergne, T., Notz, D., Pedersen, L. T., Tonboe, R. T., Saldo, R., and Sørensen, A. M.: Satellite passive microwave sea-ice concentration data set intercomparison: closed ice and ship-based observations, *The Cryosphere*, 13, 3261–3307, <https://doi.org/10.5194/tc-13-3261-2019>, 2019.
- Kern, S., Lavergne, T., Notz, D., Pedersen, L. T., and Tonboe, R.: Satellite passive microwave sea-ice concentration data set inter-comparison for Arctic summer conditions, *The Cryosphere*, 14, 2469–2493, <https://doi.org/10.5194/tc-14-2469-2020>, 2020.
- Meier, W., Fetterer, F., Savoie, M., Mallory, S., Duerr, R., and Stroeve, J.: NOAA/NSIDC Climate Data Record of Passive Microwave Sea Ice Concentration, Version 3, NSIDC: National Snow and Ice Data Center, Boulder, Colorado, USA, <https://doi.org/10.7265/N59P2ZTG>, 2017.
- Parkinson C.L. A 40-y record reveals gradual Antarctic sea ice increases followed by decreases at rates far exceeding the rates seen in the Arctic, *PNAS*, 116 (29) (2019), pp. 14414–14423, 2019.
- Peng, G., Meier, W. N., Scott, D. J., and Savoie, M. H.: A long-term and reproducible passive microwave sea ice concentration data record for climate studies and monitoring, *Earth Syst. Sci. Data*, 5, 311–318, <https://doi.org/10.5194/essd-5-311-2013>, 2013.
- Strong, C. and Golden, K. M.: Filling the Polar Data Gap in Sea Ice Concentration Fields Using Partial Differential Equations, *Remote Sens.*, 8, 442, <https://doi.org/10.3390/rs8060442>, 2016.

8 Appendix A: Missing dates

SICCI-HR-SIC generally covers the period from 01.01.1991 to 31.12.2020, daily. Table 6 lists the dates with no product due to lack of satellite data. Most missing dates are in year 1991 when only one SSM/I mission with near-90 GHz imagery (F10) is available (Figure 1).

Year	Missing CDR dates
<i>SSM/I</i>	
1991	01-06/01, 12-13/01, 02-07/02, 10-11/02, 10/03, 27-31/03, 01-17/04, 28-30/07, 21/09, 6-11/12, 14-17/12
2000	01/12
<i>SSMIS</i>	
	None

Table 6: Dates with no SICCI-HR-SIC product due to lack of satellite imagery data.